Final Report VTRC 10-R24

Virginia Transportation Research Council

research report

Short-Term Evaluation of a Bridge Cable Using Acoustic Emission Sensors

http://www.virginiadot.org/vtrc/main/online_reports/pdf/10-r24.pdf

DEVENDRA S. PARMAR, Ph.D.
Research Professor
Department of Electrical Engineering
School of Engineering and Technology
Hampton University

STEPHEN R. SHARP, Ph.D., P.E.
Research Scientist
Virginia Transportation Research Council

Virginia Transportation Research Council, 530 Edgemont Road,
Charlottesville, VA 22903-2454, www.vtrc.net, (434) 293-1900

Standard Title Page - Report on Federally Funded Project

1. Report No.: FHWA/VTRC 10-R24	2. Government Accession No.:	3. Recipient's Catalog No.:
4. Title and Subtitle: Short-Term Evaluation of a Bridge Cable Using Acoustic Emission Sensors		5. Report Date: May 2010
		6. Performing Organization Code:
7. Author(s): Devendra S. Parmar, Ph.D., and Stephen R. Sharp, Ph.D., P.E.		8. Performing Organization Report No.: VTRC 10-R24
9. Performing Organizations and Addresses: Virginia Transportation Research Council 530 Edgemont Road Charlottesville, VA 22903 Hampton University 168 Marshall Avenue Hampton, VA 23668		10. Work Unit No. (TRAIS): 11. Contract or Grant No.: 87679/87582
12. Sponsoring Agencies' Name and Address: Virginia Department of Transportation 1401 E. Broad Street Richmond, VA 23219 Federal Highway Administration 400 North 8th Street, Room 750 Richmond, VA 23219-4825		13. Type of Report and Period Covered: Final 14. Sponsoring Agency Code:
15. Supplementary Notes:		

16. Abstract:

The Varina-Enon Bridge carries I-295 across the James River and crosses over the shipping channel that leads to the Richmond (Virginia) Marine Terminal. The bridge is a cable-stayed bridge that was opened to traffic in July 1990. It has 150 ft of vertical navigational clearance and 630 ft of horizontal navigational clearance. The overall bridge length is 4,686 ft. The bridge has six lanes (three each way) with full right and left shoulders.

This study used acoustic emission (AE) to assess the condition of strands by examining for active defects (such as corrosion, crack expansion and rubbing, wire breaks, and similar active defects) on a single stay-cable, from anchorage point to anchorage point, of the Varina-Enon Bridge. Testing was performed over short durations of time during periods that included low traffic volumes (acoustically quiet) and high traffic volumes (acoustically noisy). In addition, computer software was used to determine the source and location of the acoustic event. The most significant finding was that AE events were being generated inside the pylon in the saddle region. Further, although AE responses from the stay-cable did not contain any signatures of rubbing from previously broken cable and/or breaking during the testing period, AE signals were detected, possibly because of higher winds or blowing debris striking the cable/anchorage region.

The study recommends that the Virginia Department of Transportation's Richmond District Bridge Division measure and map the cracks in the northern and southern stay-cable pylons of the bridge; evaluate the northern pylon saddle regions using AE and determine which areas show the greatest acoustical activity; evaluate the stay-cable anchorage regions more closely using AE; and determine the source of the AE signal that was detected during this study. Finally, the anchorage regions should be evaluated, and VDOT should consider using AE periodically to evaluate the health of this structure and determine which regions are exhibiting significant AE activity. Regions with elevated AE activity should take precedence over non-active regions during inspection.

17 Key Words: acoustic emission, corrosion, cable, nondestructive, cracking		18. Distribution Statement: No restrictions. This document is available to the public through NTIS, Springfield, VA 22161.	
19. Security Classif. (of this report): Unclassified	20. Security Classif. (of this page): Unclassified	21. No. of Pages: 30	22. Price:

FINAL REPORT

SHORT-TERM EVALUATION OF A BRIDGE CABLE USING ACOUSTIC EMISSION SENSORS

Devendra S. Parmar, Ph.D.
Research Professor
Department of Electrical Engineering
School of Engineering and Technology
Hampton University

Stephen R. Sharp, Ph.D., P.E.
Research Scientist
Virginia Transportation Research Council

In Cooperation with the U.S. Department of Transportation
Federal Highway Administration

Virginia Transportation Research Council
(A partnership of the Virginia Department of Transportation
and the University of Virginia since 1948)

Charlottesville, Virginia

May 2010
VTRC 10-R24

DISCLAIMER

The contents of this report reflect the views of the authors, who are responsible for the facts and the accuracy of the data presented herein. The contents do not necessarily reflect the official views or policies of the Virginia Department of Transportation, the Commonwealth Transportation Board, or the Federal Highway Administration. This report does not constitute a standard, specification, or regulation. Any inclusion of manufacturer names, trade names, or trademarks is for identification purposes only and is not to be considered an endorsement.

Copyright 2010 by the Commonwealth of Virginia.
All rights reserved.

ABSTRACT

The Varina-Enon Bridge carries I-295 across the James River and crosses over the shipping channel that leads to the Richmond (Virginia) Marine Terminal. The bridge is a cable-stayed bridge that was opened to traffic in July 1990. It has 150 ft of vertical navigational clearance and 630 ft of horizontal navigational clearance. The overall bridge length is 4,686 ft. The bridge has six lanes (three each way) with full right and left shoulders.

This study used acoustic emission (AE) to assess the condition of strands by examining for active defects (such as corrosion, crack expansion and rubbing, wire breaks, and similar active defects) on a single stay-cable, from anchorage point to anchorage point, of the Varina-Enon Bridge. Testing was performed over short durations of time during periods that included low traffic volumes (acoustically quiet) and high traffic volumes (acoustically noisy). In addition, computer software was used to determine the source and location of the acoustic event. The most significant finding was that AE events were being generated inside the pylon in the saddle region. Further, although AE responses from the stay-cable did not contain any signatures of rubbing from previously broken cable and/or breaking during the testing period, AE signals were detected, possibly because of higher winds or blowing debris striking the cable/anchorage region.

The study recommends that the Virginia Department of Transportation's Richmond District Bridge Division measure and map the cracks in the northern and southern stay-cable pylons of the bridge; evaluate the northern pylon saddle regions using AE and determine which areas show the greatest acoustical activity; evaluate the stay-cable anchorage regions more closely using AE; and determine the source of the AE signal that was detected during this study. Finally, the anchorage regions should be evaluated, and VDOT should consider using AE periodically to evaluate the health of this structure and determine which regions are exhibiting significant AE activity. Regions with elevated AE activity should take precedence over non-active regions during inspection.

FINAL REPORT

SHORT-TERM EVALUATION OF A BRIDGE CABLE USING ACOUSTIC EMISSION SENSORS

Devendra S. Parmar, Ph.D.
Research Professor
Department of Electrical Engineering
School of Engineering and Technology
Hampton University

Stephen R. Sharp, Ph.D., P.E.
Research Scientist
Virginia Transportation Research Council

INTRODUCTION

The use of acoustic emission (AE) technology for nondestructive testing (NDT) of highway bridges can provide field-proven technology for improved inspection procedures; reduce or eliminate unnecessary maintenance; reduce uncertainty in decision-making; reduce inspection frequency; extend bridge life; quantify damages; and thus predict remaining service life, all of which can save lives, money, and time.

AEs are generated by a sudden release of energy from a localized source such as the extension of a crack in a stressed material, crack growth, and crack propagation in a high-stressed zone adjacent to the tip of a crack. The basic principle involved in AE measurement is the change in propagation parameters of a wave signal through a medium. These changes in signals are amplified with the help of resonant piezoelectric devices. The amplified signal looks different in comparison to the emitted signal. By measuring the signal parameters such as counts, amplitude, duration, rise time, and energy counts (the area under the rectified signal envelope), a great deal of quantitative information on the magnitude of material defects, location and time of their origination, and rate of their propagation is obtained. These signal-related parameters and the description of hits (i.e., AE events) that includes the external parameters such as the current value of the applied load, time of detection, cycle count during the fatigue, and level of continuous background noise at the time of detection are fed into a computer for analysis. Based on the output from this analysis, more informed decisions could be made about the condition and health of critical structural components.

Highway bridges are crucial components of a healthy and productive transportation infrastructure. A variety of factors may lead to their degradation. Cracks and flaws in bridge components may have originated during the fabrication or construction process. These imperfections can then grow because of traffic fatigue, corrosion, or both. Load, environment, and corrosion loss affect the performance and cause deterioration. Concrete bridge components in long-term service suffer from degradation caused by corrosion of reinforcement, which can

reduce the cross section of the steel and damage the bulk concrete. The actual cause of deterioration of highway bridge structural components is a complex combination of factors that include material characteristics, load, and environment. Such factors result in damage through processes such as development of cracks, their growth, bridge structural member plastic/elastic deformations, and active corrosion, any or all of which can function as an AE source.

The Varina-Enon Bridge is a cable-stayed bridge that carries I-295 across the James River in Virginia. It has 150 ft of vertical navigational clearance and 630 ft of horizontal navigational clearance. From the surface of the James River to the top of the northern pylon is approximately 300 ft. The bridge has six lanes (three each way) with full right and left shoulders and an overall length of 4,686 ft when measured from the back of each backwall.

Not only is the size of this bridge a challenge for inspection, however, the position of important bridge features is as well. Further, the inspection of some of the steel features can be difficult because they are either embedded in concrete, encased in plastic, or both. The bridge is regularly inspected every 24 months in accordance with federal guidelines. These guidelines, however, do not require the use of AE in the inspection. Therefore, with such a sizable and challenging structure to inspect, this study used AE to evaluate a single stay-cable of the Varina-Enon Bridge and the saddle area the cable crosses. It was expected that this approach would prove beneficial for the Virginia Department of Transportation (VDOT), which inspects and maintains the bridge, while demonstrating the benefit of this nondestructive technique.

PURPOSE AND SCOPE

The purpose of this study was to determine if short-term monitoring with AE instrumentation could assess the condition of strands by examining for active defects (such as corrosion, crack expansion and rubbing, breaks, and similar active defects) on a single stay-cable from anchorage point to anchorage point. The scope of the evaluation was Stay-cable No. 10 (hereinafter Cable 10) on the Varina-Enon Bridge (VA Structure 2907, Federal ID 10007) and the saddle area Cable 10 crosses inside the northern pylon (Pylon No. 17).

Monitoring was performed during periods of low traffic volumes (acoustically quiet) and high traffic volumes (acoustically noisy) as well as during periods with the highest and lowest ambient temperatures on the bridge. A secondary purpose was to use the measured AE signals to pinpoint regions of greater acoustic activity that might require more in-depth inspections.

METHODS

The supporting stay-cables of the Varina-Enon Bridge contain steel strands made up of individual wires. To evaluate these wires, a 16-channel AE system was procured. Using 16 AE sensors, Cable 10 was monitored on the bridge, which is shown in Figure 1.

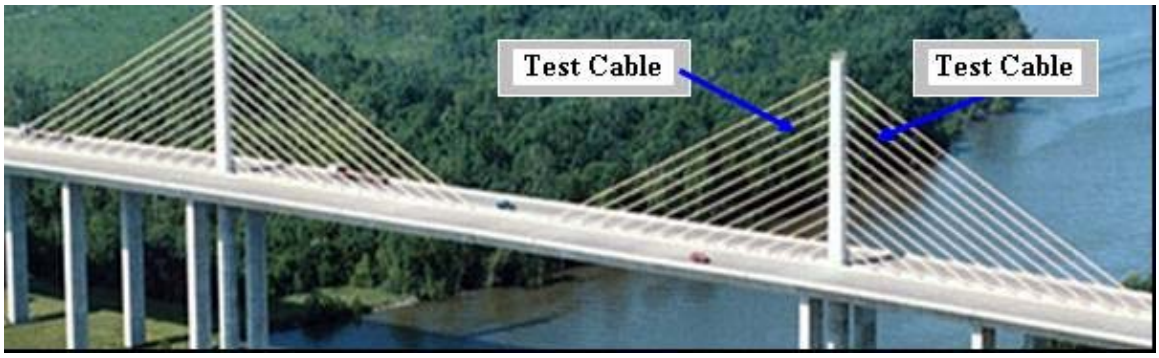

Figure 1. Varina-Enon Bridge and Test Cable (Fourth Cable From Top) Supported by Northern Pylon

Sensor Installation and Locations

During sensor installation, an aerial work platform was used to access various predetermined installation points along Cable 10, as shown in Figure 2. AE sensors (R0.45I-LP-SC-5 4.5 kHz low power sensors designed for outdoor use) were affixed with epoxy at these predetermined locations on the cable. Fastener straps secured the sensors in place and provided additional protection from various environmental factors. The inside pylon access ladder helped in installing the sensors along the length of the cable that lies in the saddle area and provided a way to relieve some of the strain on each cable by providing attachment points along the ladder. A dedicated cable connected each sensor to the data acquisition (DAQ) system. A broadband wireless system used in conjunction with the DAQ system transmitted the data remotely to Hampton University for analysis. For this study, the DAQ system selected was the Sensor Highway II (a self-contained industrial system in a NEMA-4 outdoor enclosure with a 16-channel motherboard and 16 bit resolution) manufactured by Physical Acoustics Corporation.

As mentioned earlier, the entire length of Cable 10, including the length that lies inside of the pylon, had 16 AE sensors installed. This stay-cable is symmetric about the northern pylon, with the horizontal distance between the pylon and the deck anchor points being 213.6 ft

Figure 2. *Left,* Overview of AE Sensor Installation at Selected Locations on Cable 10; *Right,* Close-Up of Installation of Single AE Sensor

on the northern and southern sides of the pylon. AE sensors were placed outside the pylon along Cable 10 and inside the pylon on the concrete structure, which encapsulates the saddle. Figure 3 is a schematic that shows Sensors 1 through 4, which are located on the north side of the cable outside the northern pylon, and Sensors 13 through 16, which are located on the south side of the cable outside the northern pylon. Table 1 gives details of sensor locations on the cable.

Sensors 5 through 12 were affixed inside the pylon on the concrete surface in the region of the saddle area. Figure 4 shows a typical example of the sensor installation in the saddle area. Sensors 5 through 8 are located on the west face of the saddle; Sensors 9 through 12 are located on its east face. Figure 5 is a schematic of the sensor locations in the saddle area. Table 2 gives details of linear locations of sensors from the highest center points, A and B, on the saddle. Table 3 gives the dimensions of the saddle opening.

The cable was monitored for 2½ months each during the winter and summer months of 2008 and 2009. This ensured that the regions being monitored were subjected to different atmospheric exposure conditions, which would allow normal temperature-related expansion and contraction to occur.

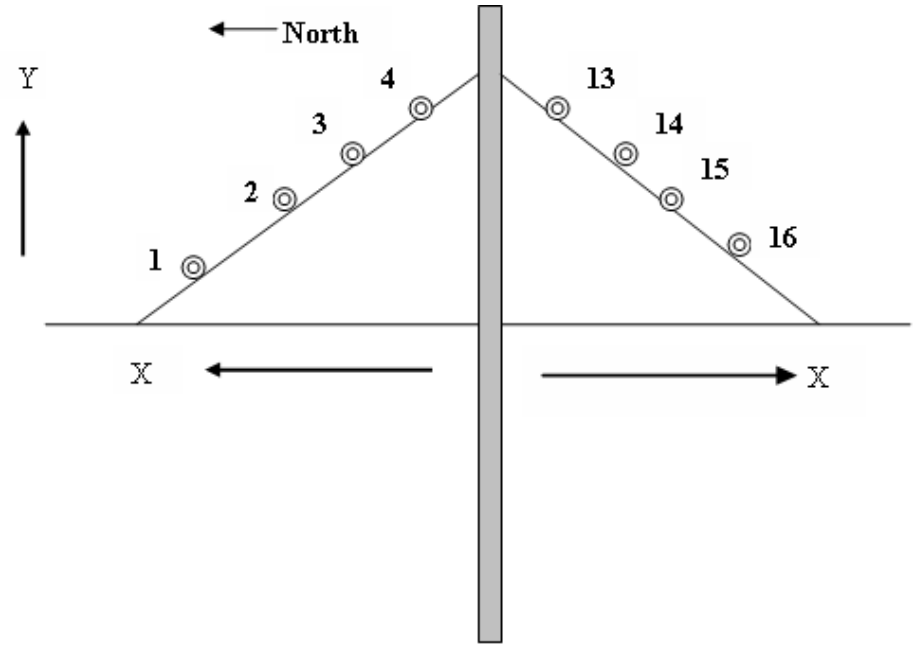

Figure 3. Side View Schematic of Sensor Locations on the Two Spans of Cable 10. See Table 6 for the X-Y coordinates.

Table 1. Linear Locations of Sensors on Cable Spans from Center of Northern Pylon

Span	Center Point	Sensor No.	Linear Horizontal Distance Along Deck from Northern Pylon (ft)	Linear Vertical Height from Deck (ft)
North	Northern pylon	1	159.00	28.07
		2	121.00	47.64
		3	83.00	67.21
		4	45.00	86.78
South	Northern pylon	13	45.00	86.78
		14	86.50	67.21
		15	121.75	47.64
		16	159.00	28.07

Figure 4. Typical Photographs of Sensors Affixed on Concrete Walls of Cable Saddle

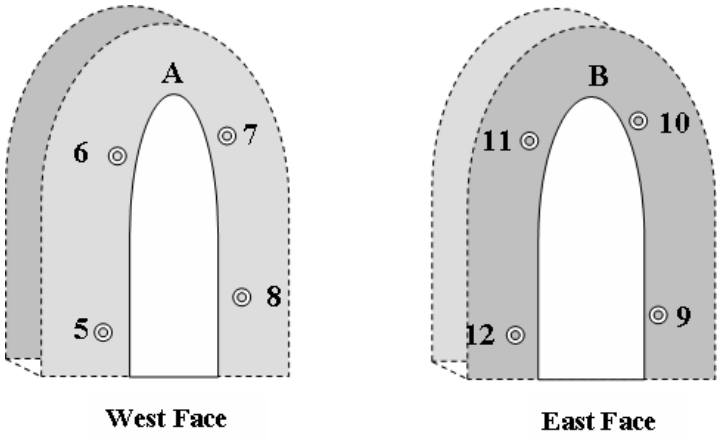

Figure 5. Schematic Showing Installed Sensor Locations in Saddle Area Such That Sensors 5, 6, 7, and 8 on West Face Are Across From Sensors 12, 11, 10, and 9, Respectively, on East Face. *A* and *B* are the highest points on the open area of the saddle.

The sensor locations on the west face run clockwise from 5 through 8 and then continue counterclockwise from 9 through 12 on the east face such that, as previously discussed, Sensors 5 through 8 on the west face are across from Sensors 12, 11, 10, and 9, respectively, on the east face. For the purpose of simplicity of analysis and interpretation of the results, linear locations of Sensors 5 through 8 on the west face were normalized with reference to Sensor 5 (Table 4) and those of Sensors 9 through 12 on the east face with reference to Sensor 12 (Table 5).

Table 2. Linear Locations of Sensors From Highest Center Points A and B on Saddle in Figure 5

Saddle Face	Center Point	Sensor No.	Linear Distance from Center Point (in)	Linear Distance from Center Point (ft)
West	A	5	57.00	4.75
		6	19.50	1.63
		7	11.00	0.92
		8	38.50	3.2
East	B	9	43.50	3.63
		10	11.25	0.94
		11	18.50	1.54
		12	56.00	4.67

Table 3. Dimensions of Saddle Opening Inside Northern Pylon

Description	Distance (in)
Width	24
Height	57
Base	75

Table 4. Linear Locations of Sensors on West Face in Reference to Sensor 5 in Figure 5

Sensor No.	Linear Distance from Sensor 5 (in)	Linear Distance from Sensor 5 (ft)
5	00.00	0.00
6	19.50	1.63
7	30.50	2.54
8	69.00	5.75

Table 5. Linear Locations of Sensors on East Face in Reference to Sensor 12 in Figure 5

Sensor No.	Linear Distance from Sensor 12 (in)	Linear Distance from Sensor 12 (ft)
12	00.00	0.00
11	18.50	1.54
10	29.75	2.48
9	73.25	6.10

Operation Procedure

The AE DAQ system runs on a battery backup installed alongside the DAQ system as shown in Figure 6. An AE signal amplitude threshold of 45 dB was set to discriminate the reliable damage-related emissions from the background noise signals. The advent of an AE event (when the AE signal amplitude is over the threshold of 45 dB), such as generation of a crack, a break, or weather-related effects resulting in AE, activates the system automatically. The AE DAQ system records the AE data consisting of the AE response parameters such as the date and time of the event, sensor response to the event, frequency of the AE, amplitude of AE,

Figure 6. Sensor Highway II DAQ System and Battery Backup

and number of hits during the event. An active broadband wireless connection then transmits the data to the server, which can be remotely located, for downloading. A linear, 2D and 3D locator software program, AEwin, plots and is used for analysis of the data. Figure 7 shows a sample 2D plot of the data representing hits, their amplitudes, and the date and times recorded October 11 through 15, 2008. The windows labeled 1 through 6 represent different AE parameters related to sensors; their locations, responses, dates, and times; and the activity levels. Table 6 provides the window definitions.

RESULTS AND DISCUSSION

AE responses from the test cable were recorded at different times from August 2008 to October 2009. This period included low traffic volumes (acoustically quiet) and high traffic volumes (acoustically noisy), as well as periods with the highest (2½ months of summer) and lowest (2½ months of winter) ambient temperatures at the bridge.

As mentioned previously, AE Sensors 1 through 4 and 13 through 16 were affixed to the plastic duct that encloses the stay-cable whereas Sensors 5 through 12 were installed on the concrete surface inside the pylon. This is important because the AE propagation through a non-metallic medium is much slower than in a metal medium.[1] In addition, the attenuation of AE signals is much stronger in a non-metallic than in a metal medium.[1] To ensure that the AE propagation from the plastic cover of the cable to the sensors was via the metal cable, ping tests were performed. AE Sensors 1 and 16, located closest to the anchorage points, were pinged, and all sensor responses were recorded. Sensors 1 through 4 responded to a ping close to Sensor 1, and Sensors 13 through 16 responded to a ping close to Sensor 16. Therefore, outside

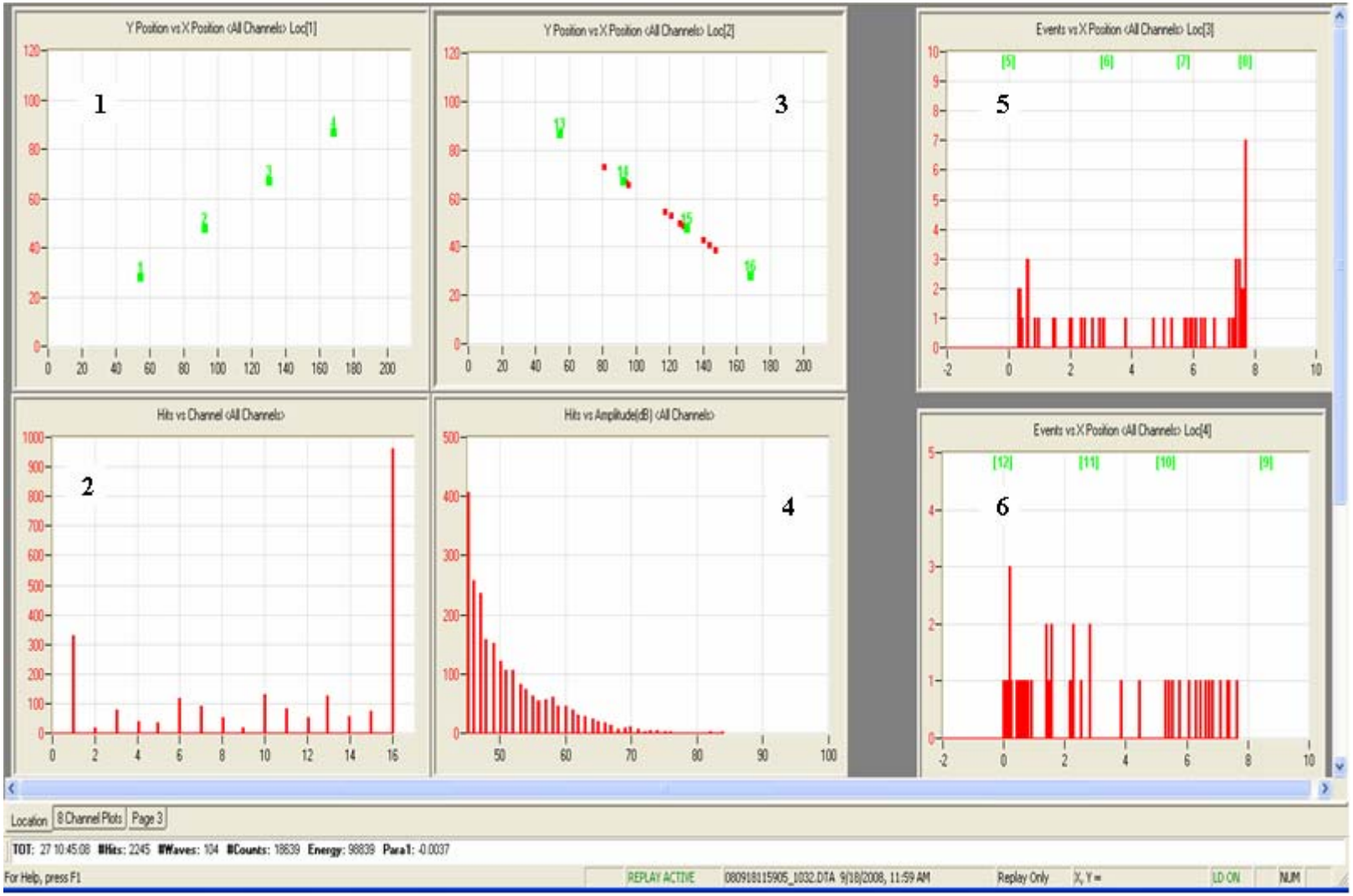

Figure 7. Sample 2D Plot of Data Representing AE Events (Hits), Their Amplitudes, and Dates and Times Recorded, October 11-15, 2008

Table 6. Definitions of Windows Labeled 1 Through 6 in Figure 7

Window No.	Definition
1	Linear X and Y locations of Sensors 1-4 on north span of cable
2	AE response of all 16 sensors
3	Linear X and Y locations of Sensors 13-16 on south span of cable
4	AE signal amplitude distribution for all sensors
5	Linear X locations and AE event responses of Sensors 5-8 on west face of saddle
6	Linear X locations and AE event responses of Sensors 9-12 on east face of saddle

environmental factors such as the AE generated by a falling raindrop on the cable propagates through the plastic sleeve to the metal cable to be detected by a sensor. However, the AE signals related to any break and/or damage to the cable strand are also measured but have different characteristic signatures.

Acoustic Emission Signatures

AE Signal Characteristics

The recorded AE signals have characteristics of the events that take place in the cable and/or saddle. These characteristics determine the source of the recorded signal. Three examples of AE signatures detected during this study are discussed here in relation to the sensors that detected the signal.

1. *AE signals related to damage of the cable strands are supposed to be dramatic.* These will have high energy, a high amplitude, and a very short duration. The AE amplitudes from Sensors 2 through 4 and 13 through 15 installed on the stay-cable, shown in Window 4 of Figure 7, are feeble and very weak, indicating an absence of any break, crack, or damage to the cable strands during the event. In fact, the responses correspond to the feeble AE sources unrelated to the cable. The weather data during the period confirmed the AE source to be the raindrops hitting the cable. The AE sensors have detected even such weaker hits. The smaller dots appearing in between the sensor installation points (larger square symbols adjacent to the sensor number) in Window 3 in Figure 7 indicate the actual locations of falling raindrops.

2. *AE signals from Sensor 1 and Sensor 16, which are the two sensors closest to the stay-cable deck anchorage points, also exhibited hits.* As shown in Window 2 of Figure 7, Sensor 1 measured more than 300 hits and Sensor 16 measured more than 900 hits during the October 11 through 15, 2008, test period. The dots in Window 3 represent locations where AE generated because of falling raindrops along the sensor installation points. The absence of dots between the sensor installation points (larger square symbols adjacent to the sensor number) in Window 1 indicates that the AE source is outside the location perimeter of Sensors 1 through 4. These responses occurred when there was no rain on the bridge and might have been the result of cable vibrations caused by higher winds or blowing debris striking the cable/anchorage region. However, confirmation of this would require further investigation.

3. *AE signals detected by Sensors 5 through 12 in the saddle area, though weak, are not weather related*. They represent AE activity in the concrete wall of the saddle. Although the AE activity is in the entire saddle structure, its intensity is higher in the north side corner of the structure near the locations of Sensors 5 and 12 and in the south side corner of the structure where Sensor 8 is located.

AE Signatures in Pylon Saddle Area

AE has detected three types of activities, consistent with cracking, in the concrete encapsulating the cable in the saddle area:

1. crack expansion (expansion of the pre-existing cracks)

2. crack formation (creation of new cracks)

3. crack rubbing (friction attributable to rubbing of the two sides of a pre-existing or newly created crack).

As a rule of thumb, the concrete crack initiation/expansion and the crack rubbing events are identified by AE signal characteristics detailed in Table 7.[2,3] Typical examples of AE responses during a cracking event are detailed in Figures 8 through 10 where the energy counts (in mV) are plotted against response times (in microseconds).

Table 7. AE Signal Characteristics During a Crack Event in Concrete

Crack Event	AE Signal Characteristic			
	Energy	**Amplitude**	**Duration**	**Rise Time**
Expansion	High	High	Short	Short
Initiation	High	High	Short	Short
Rubbing/Friction	Low	Low	Longer	Longer

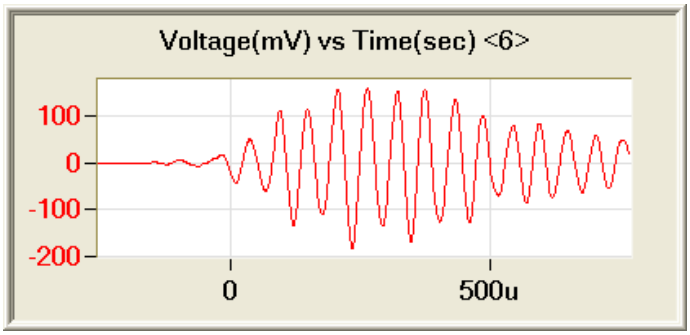

Figure 8. AE Event Representing Pre-Existing Concrete Crack Rubbing Recorded by Sensor 6

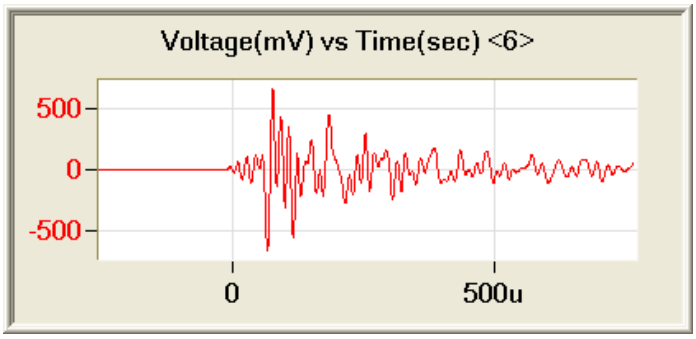

Figure 9. AE Event Representing Pre-Existing Concrete Crack Rubbing Followed by High Energy Counts of Short Duration Representing Initiation of Crack (Crack Expansion) Recorded by Sensor 6

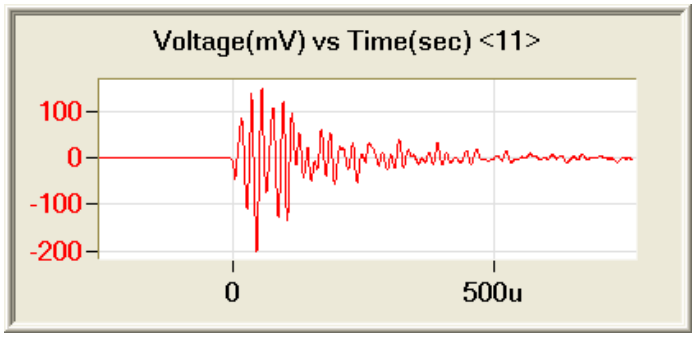

Figure 10. AE Event Representing Initiation of Concrete Crack Followed by Rubbing (Friction) Recorded by Sensor 11

The walls of a pre-existing crack in concrete near Sensor 6, mounted on the west face of the saddle, rub against each other, producing long-duration (~ 750 microseconds) but low-energy counts (up to ~±180 mV) during an event shown in Figure 8. Figure 9 shows another event representing crack rubbing followed by crack expansion demonstrated by short-duration (~75 microseconds) high-energy (up to ~±680 mV) counts recorded by Sensor 6. An AE event representing initiation of a higher energy (up to ~±200 mV) but shorter duration (~100 microseconds) micro crack followed by a longer duration (~ 400 microseconds) crack rubbing is shown in Figure 10. In all such cases, crack rubbing has been prominent and has been a common feature in crack expansion and crack initiation. New crack formation has invariably been found to be followed by crack rubbing.

Locating Acoustic Emission Points of Origin in Pylon Saddle Area

Overview

The AE signals were also evaluated to estimate the location of the AE activity as the AE system time stamps each received signal. Thus, an estimate can be made using the speed of sound in a given material. For this study, 2D AE analysis located the AE activity in the bulk of concrete of the saddle area. 3D AE analysis found a similar result from the data in Figure 7.

AE linear, 2D, and 3D data analysis has not detected any activity in the stay-cable portion located outside the pylon. However, based on the AE responses from sensors located in the

saddle area, a variety of activity in concrete structure has been detected. Some typical AE responses from Sensors 5 through 8 on the west face (Figure 11) and 9 through 12 on the east face (Figure 12) are reported here.

Figures 11 and 12 show intense AE activity across the center of the saddle region. Sensors 6 and 11 are located near the center of the saddle on its west and the east faces, respectively (Figures 11 and 12). The most likely source of this activity is the initiation of a new crack or growth of a pre-existing crack. AE signal signatures and data analysis show the presence of both. The dates and times of the activities in Figures 11 and 12 are shown in Figure 13, where the number of hits is plotted against the date and time of occurrence on August 28 and

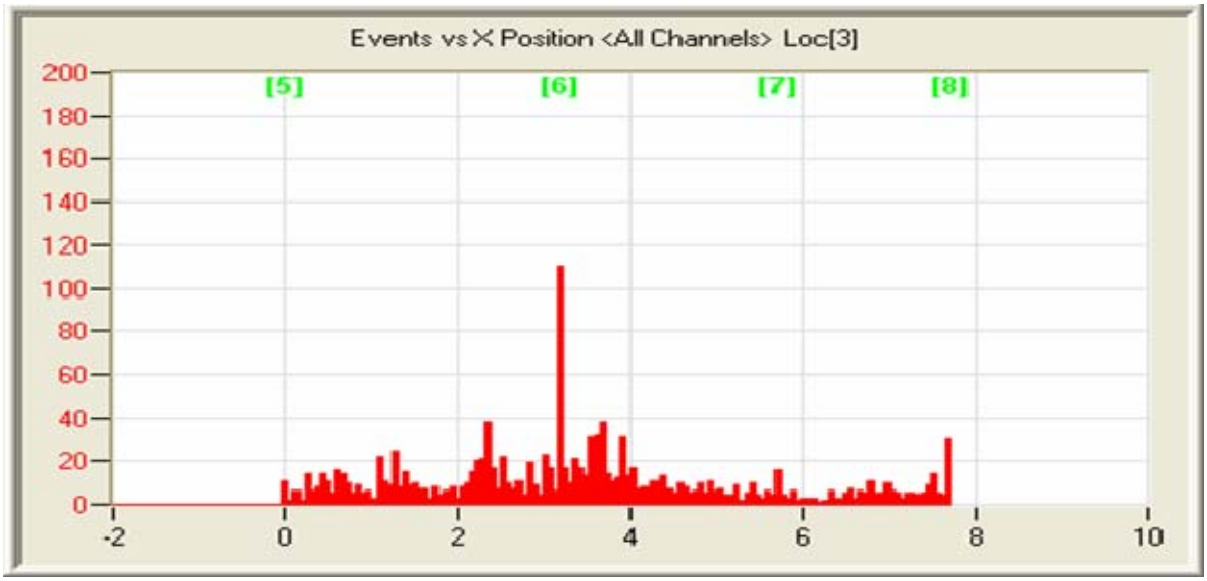

Figure 11. AE Events Recorded by Sensors 5-8, August 12-September 25, 2008

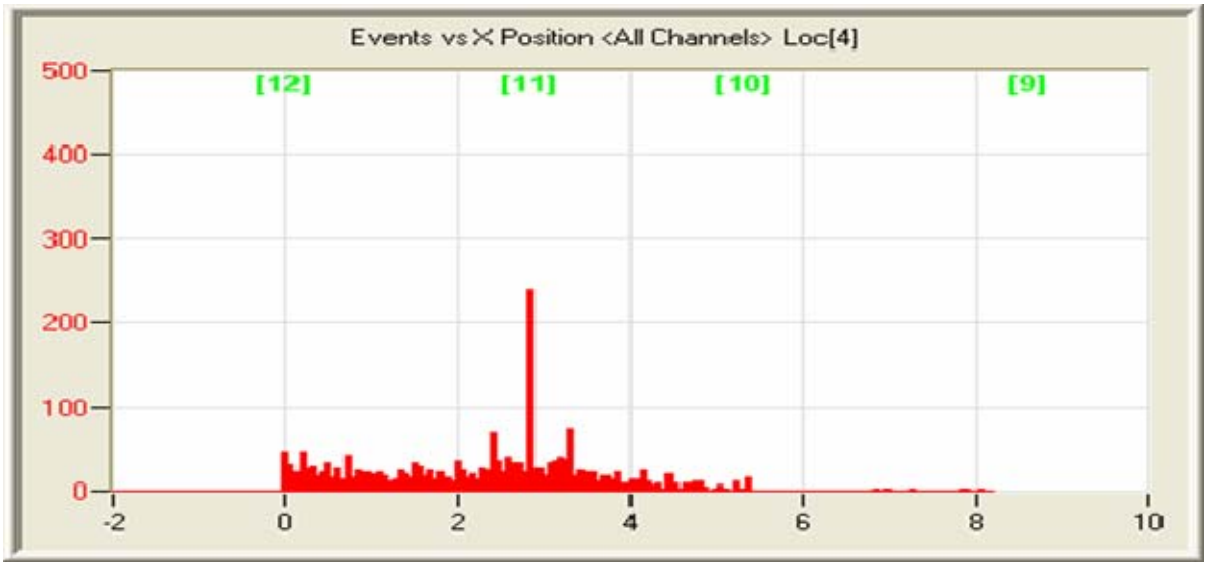

Figure 12. AE Events Recorded by Sensors 9-12, August 12-September 25, 2008

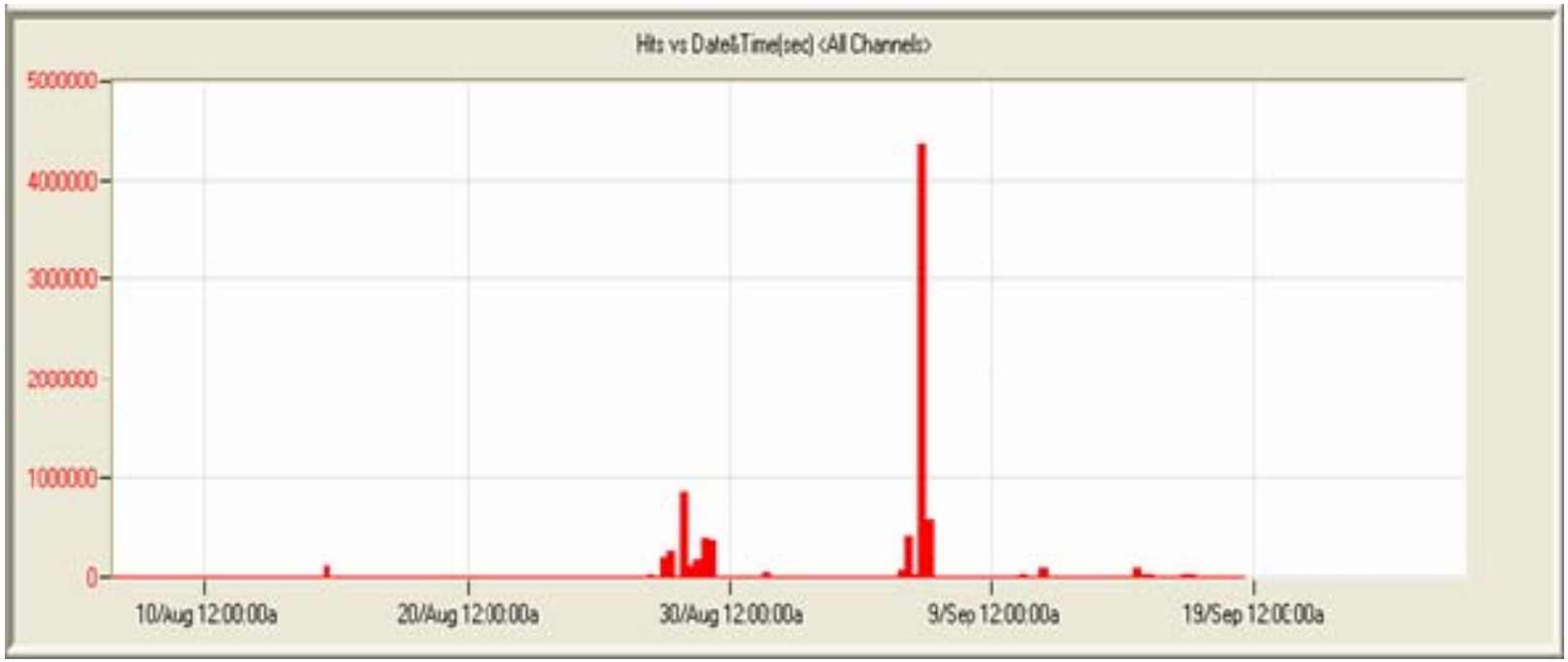

Figure 13. AE Events recorded by All Sensors, August 12-September 25, 2008. The number of hits is plotted here as a function of dates and times.

29, 2008, and September 6 through 8, 2008. AE events also occurred October 25 through 27, 2008, as shown in Figures 14 and 15, which show activities in the center and northeast corner of the saddle. From December 11, 2008, to January 29, 2009, there was AE activity in the southwest and northeast corner areas of the saddle, as shown in Figures 16 and 17, respectively.

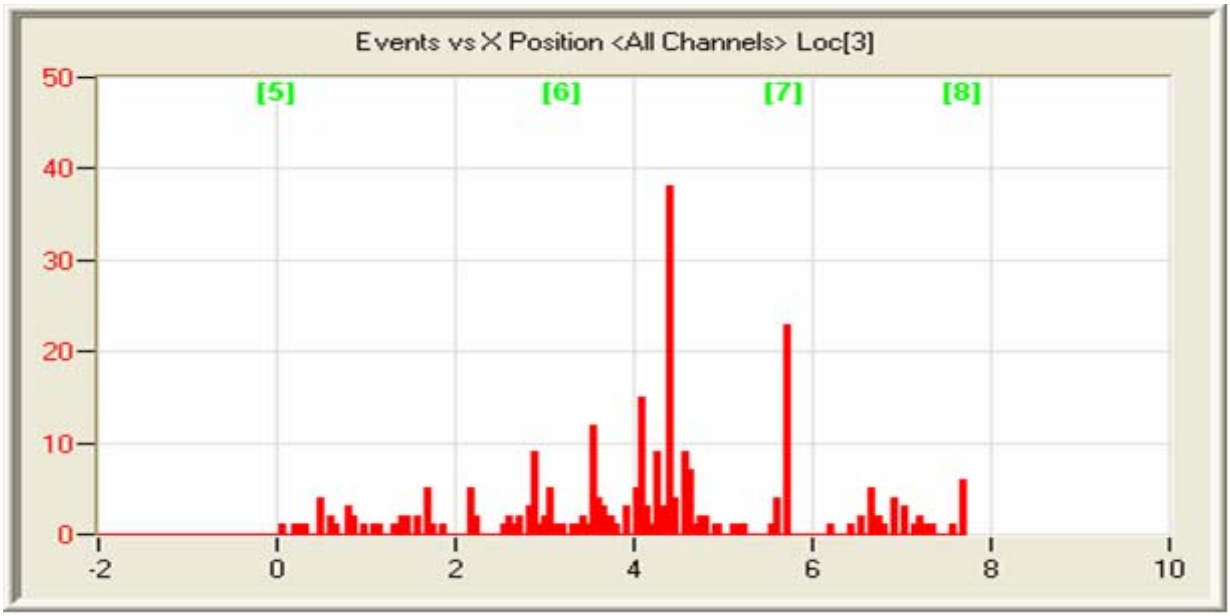

Figure 14. AE events Recorded by Sensors 5-8, October 25-27, 2008

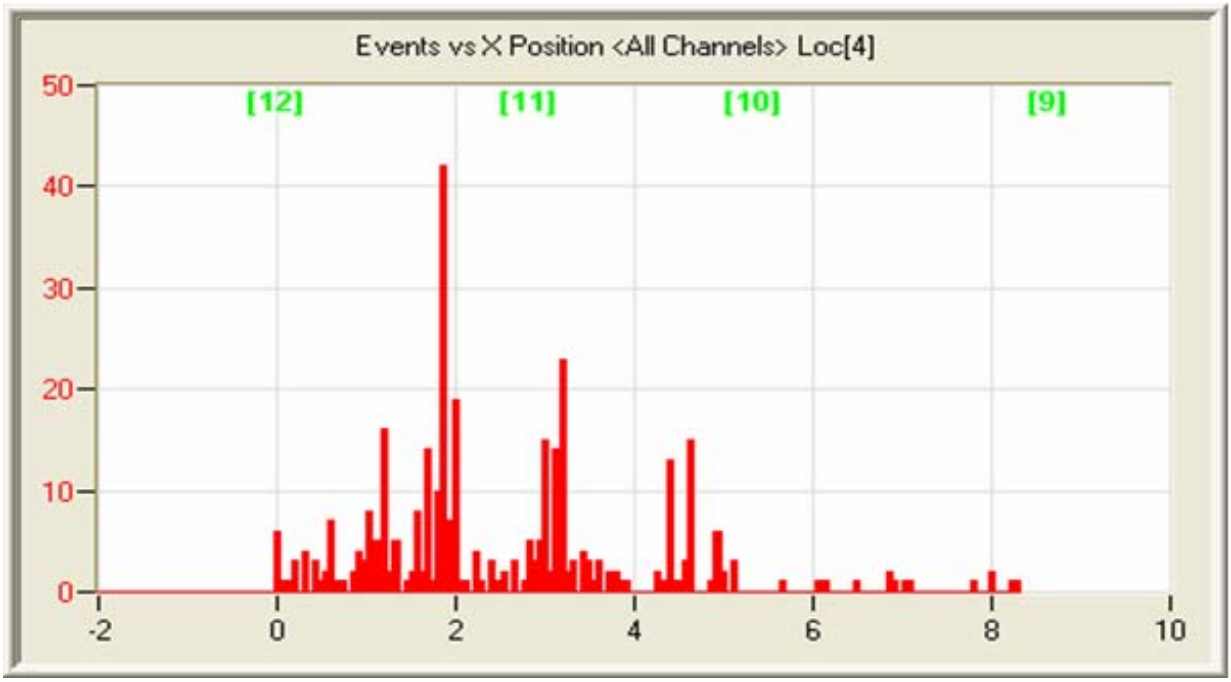

Figure 15. AE Events Recorded by Sensors 9-12, October 25-27, 2008

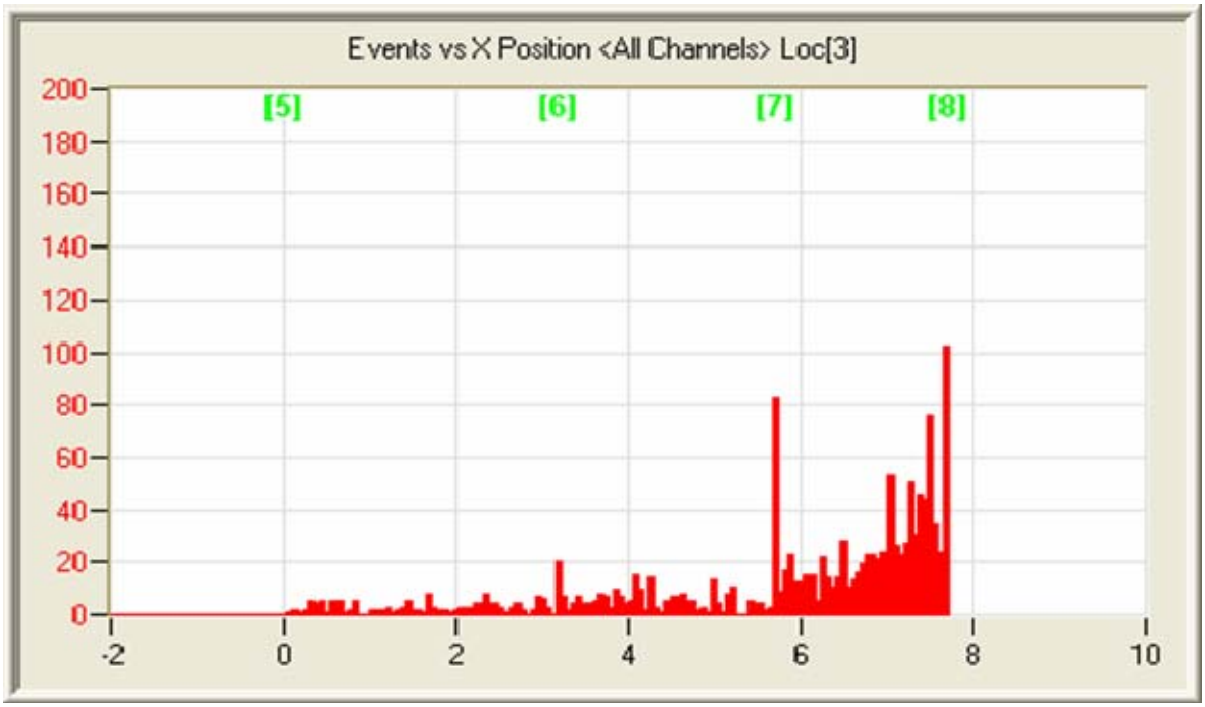

Figure 16. AE Events Recorded by Sensors 5-8, December 11, 2008-January 29, 2009

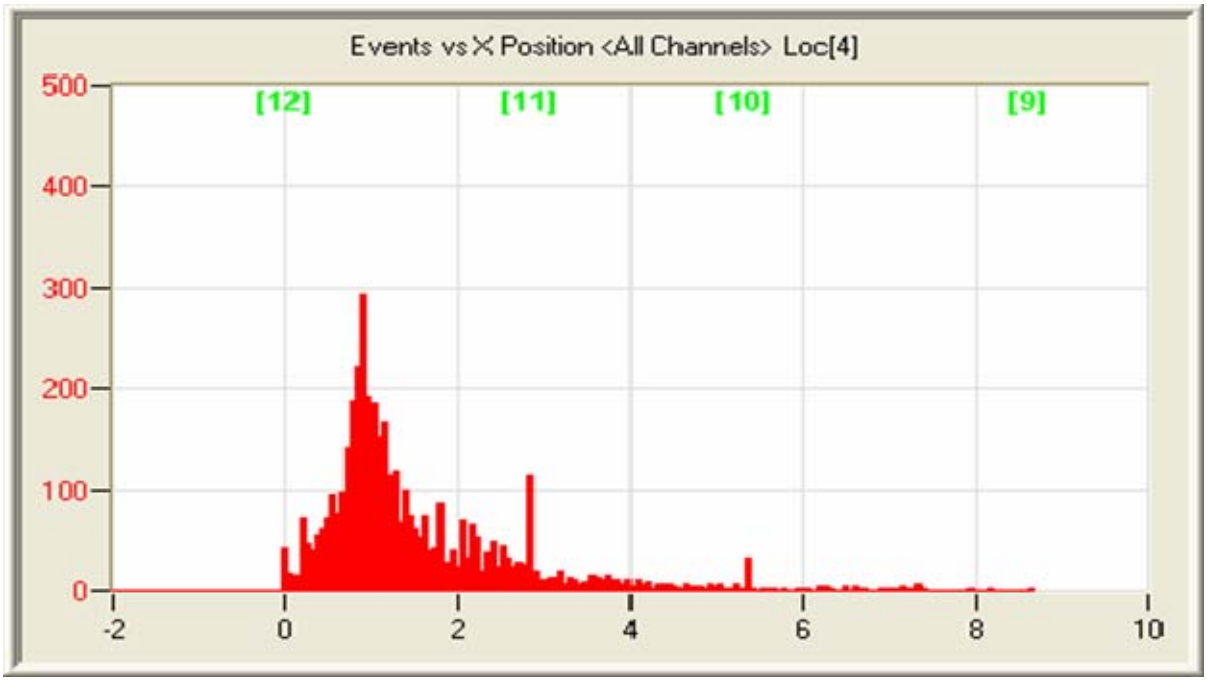

Figure 17. AE Events Recorded by Sensors 9-12, December 11, 2008-January 29, 2009

Figures 18 and 19 represent AE activities that occurred February 26 through March 6, 2009, in the northeast and northwest areas of the saddle, respectively. This was also the period of extreme cold on the bridge. Figures 20 and 21 similarly represent the AE activity that occurred September 28 through 30, 2009, in the center and north areas of the saddle walls, respectively. Data presented in Figures 11 through 21 are only typical examples, although similar AE events

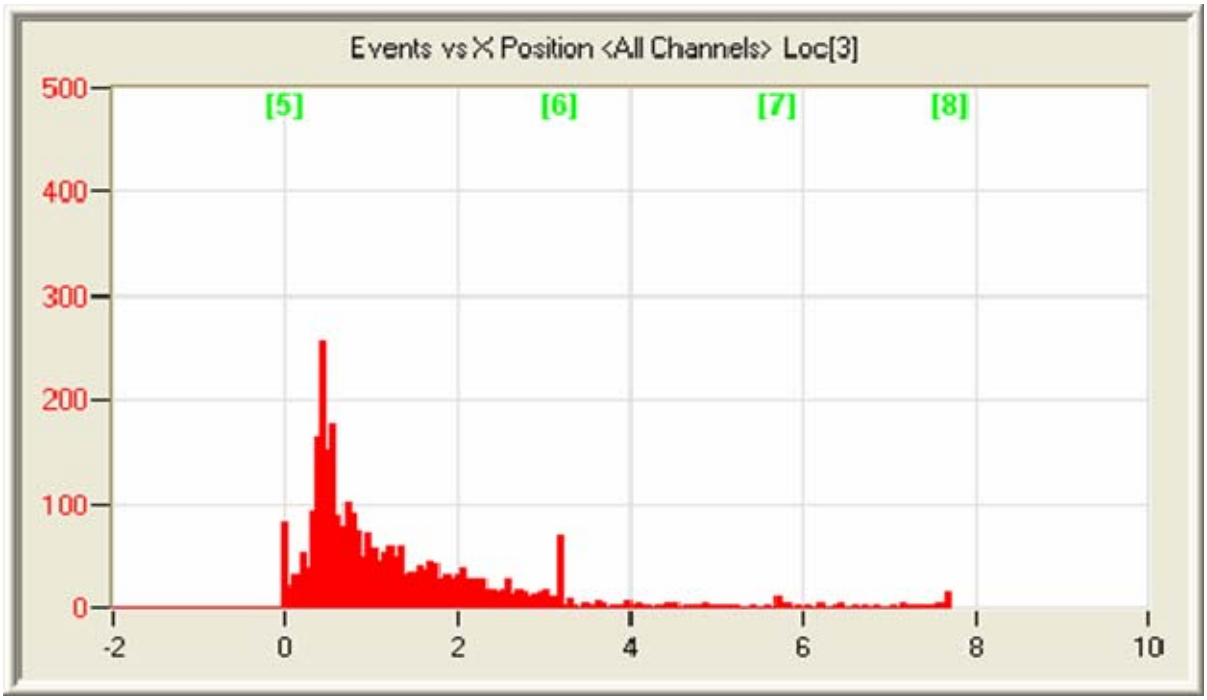

Figure 18. AE Events Recorded by Sensors 5-8, February 26-March 6, 2009 (Extreme Cold)

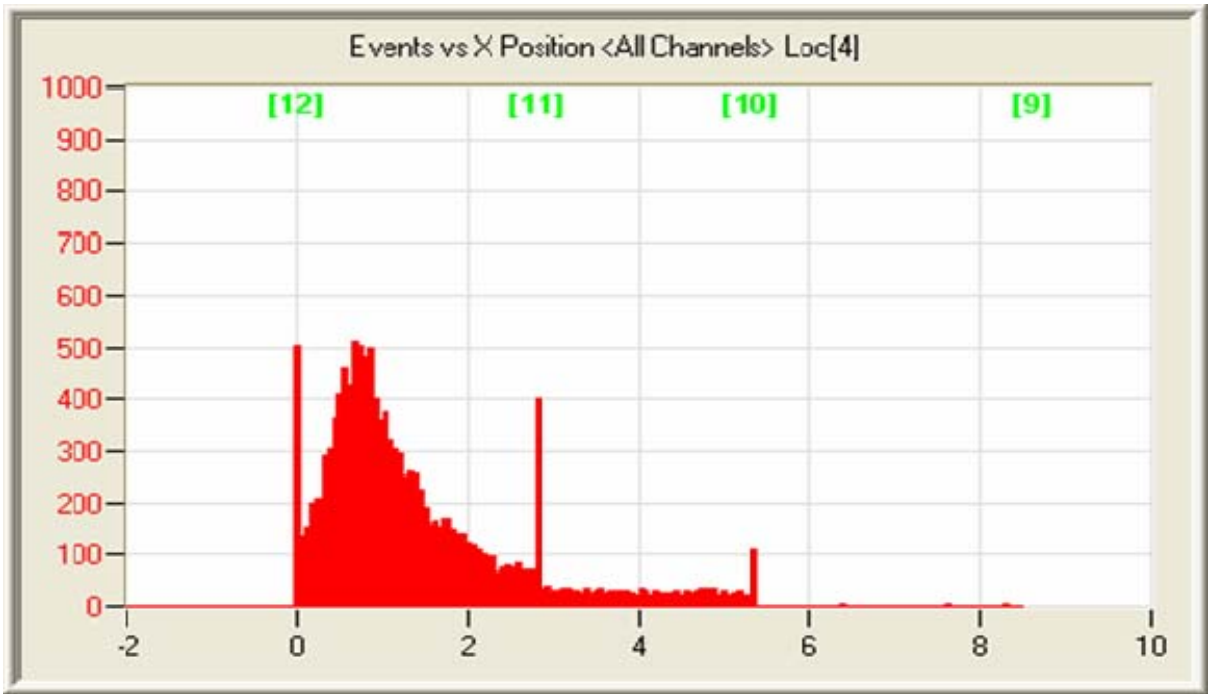

Figure 19. AE Events Recorded by Sensors 9-12, February 26-March 6, 2009 (Extreme Cold)

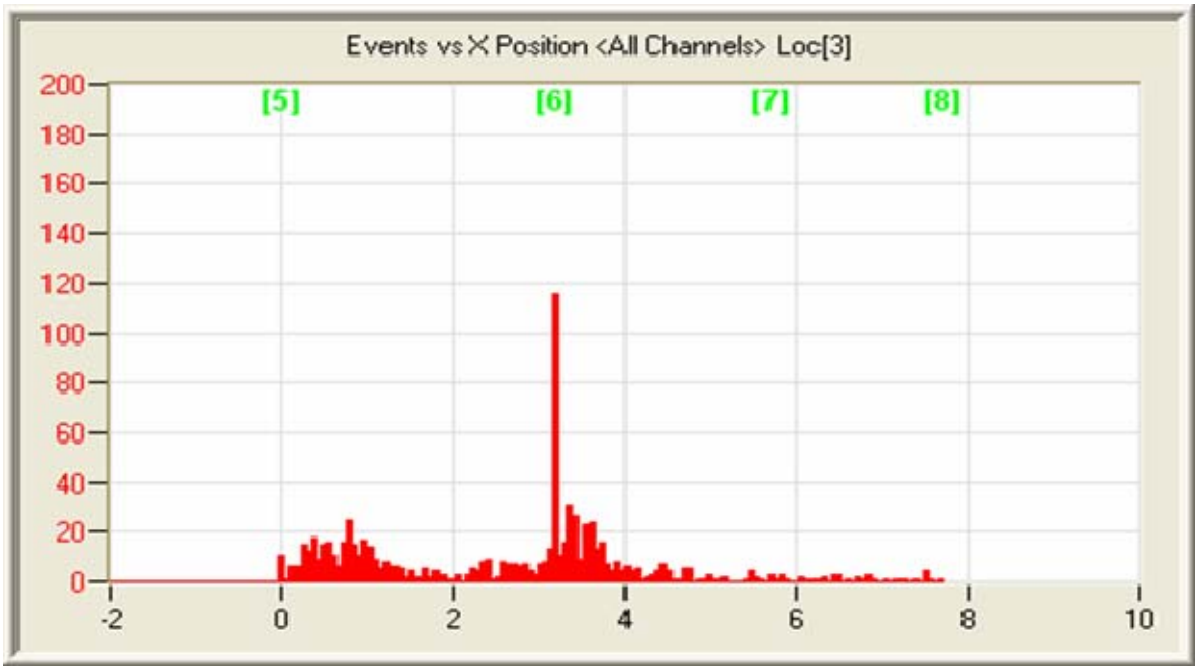

Figure 20. AE Events Recorded by Sensors 5-8, September 28-30, 2009

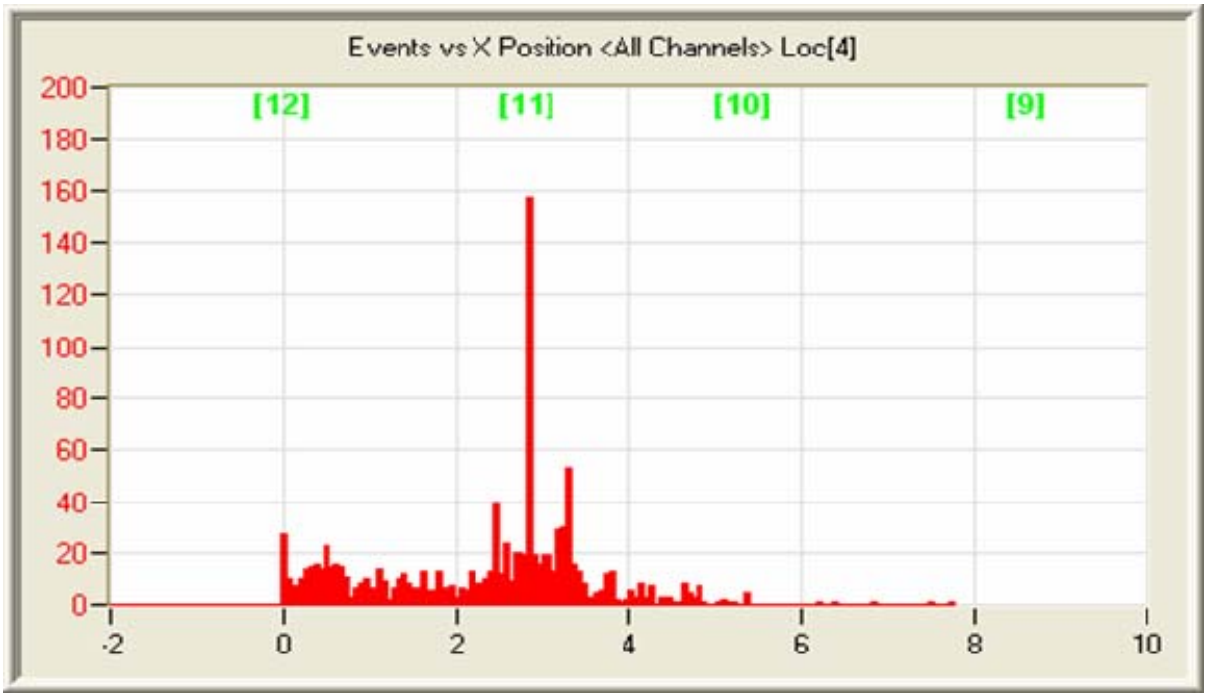

Figure 21. AE Events Recorded by Sensors 9-12, September 28-30, 2009

occurred during the entire period for which data were recorded. Since each AE event was different, plotting of the cumulative effects of all the events was avoided to avoid the loss of AE signatures corresponding to a particular event.

3D Analysis for Concrete Crack Distribution in Pylon Saddle Area

For best results from 3D software, any 2D planar groups of sensors using 3D coordinates need be confined to just one face of the test structure. Parallel sensors on an opposing face could appear as duplicate sensors with identical coordinates when the third coordinate is ignored. In this study, the width of the saddle arch (2 ft) was used as the third coordinate for 3D analysis. Table 8 gives the sensor coordinates determined from their locations in Table 2 and using the reference frame of Figure 22. The sensor locations on the west and east faces are not exactly parallel but are not on ideal locations for 3D analysis. Further, the open space under the saddle is also not ideal for the best results from 3D analysis as the AE signals traverse the open space, affecting results. However, a 3D analysis for the purpose of location estimates has been possible to determine crack-affected areas. Figures 23 and 24 show typical 3D plots of crack-related AE events. Figure 23 shows a 3D plot of the crack-related hits recorded during the summer period of August 12 through September 25, 2008. These results are in conformity with the AE event plots of Figures 8 and 9. Similarly, Figure 24 shows a 3D plot of the crack-related hits recorded during the winter period of November 13 through December 13, 2008.

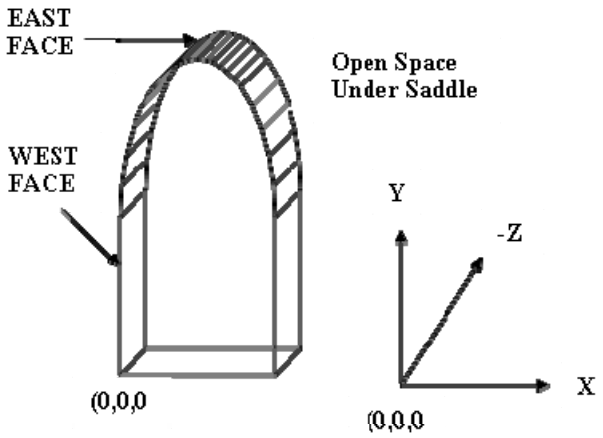

Figure 22. Frame of Reference Used for Determining Sensor Coordinates in Table 8. The origin of the frame (0,0,0) is at the northwest corner of the west face open space under the saddle arch.

Table 8. AE Sensor Coordinates Used for 3D Analysis

Sensor No.	Coordinates (in ft)		
	X	Y	Z
5	0.583	0.583	0.000
6	2.210	3.330	0.000
7	4.250	4.170	0.000
8	5.540	2.000	0.000
9	6.420	0.670	2.000
10	4.750	3.500	2.000
11	2.670	4.000	2.000
12	1.670	1.580	2.000

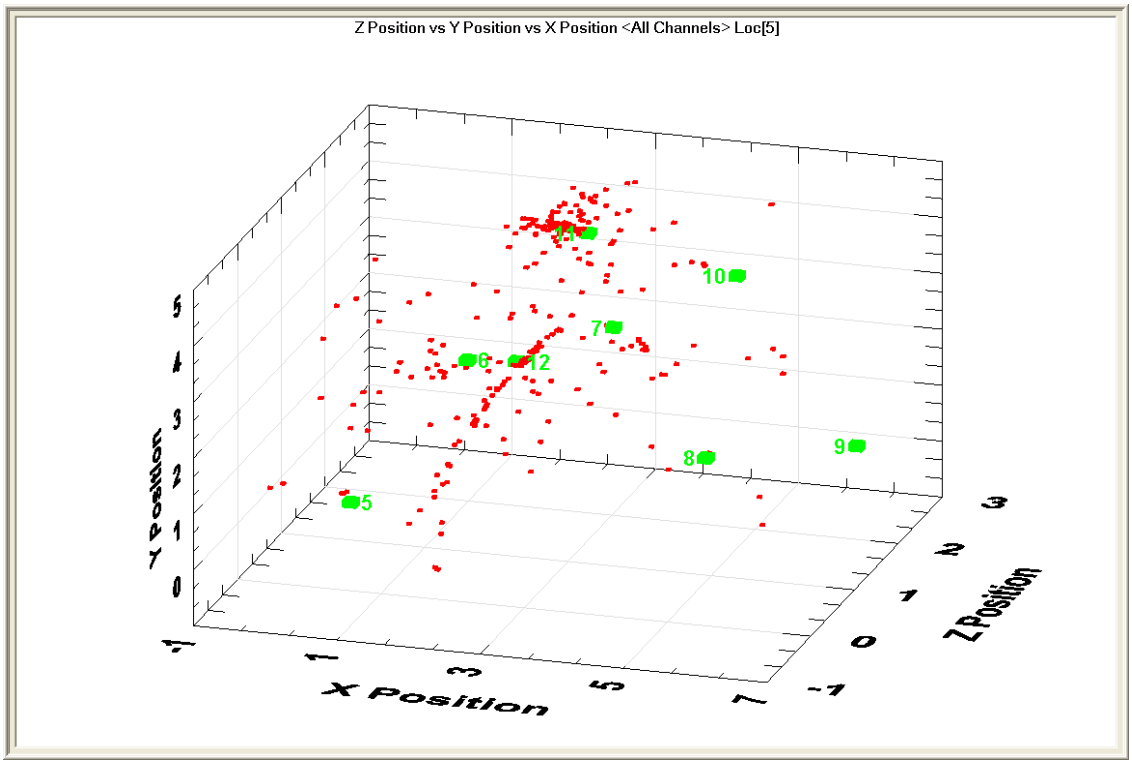

Figure 23. 3D Plot of Crack-Related AE Hits Recorded August 12-September 25, 2008, in Concrete Structure Under Cable Saddle. The coordinates (X,Y,Z) are defined in Figure 22.

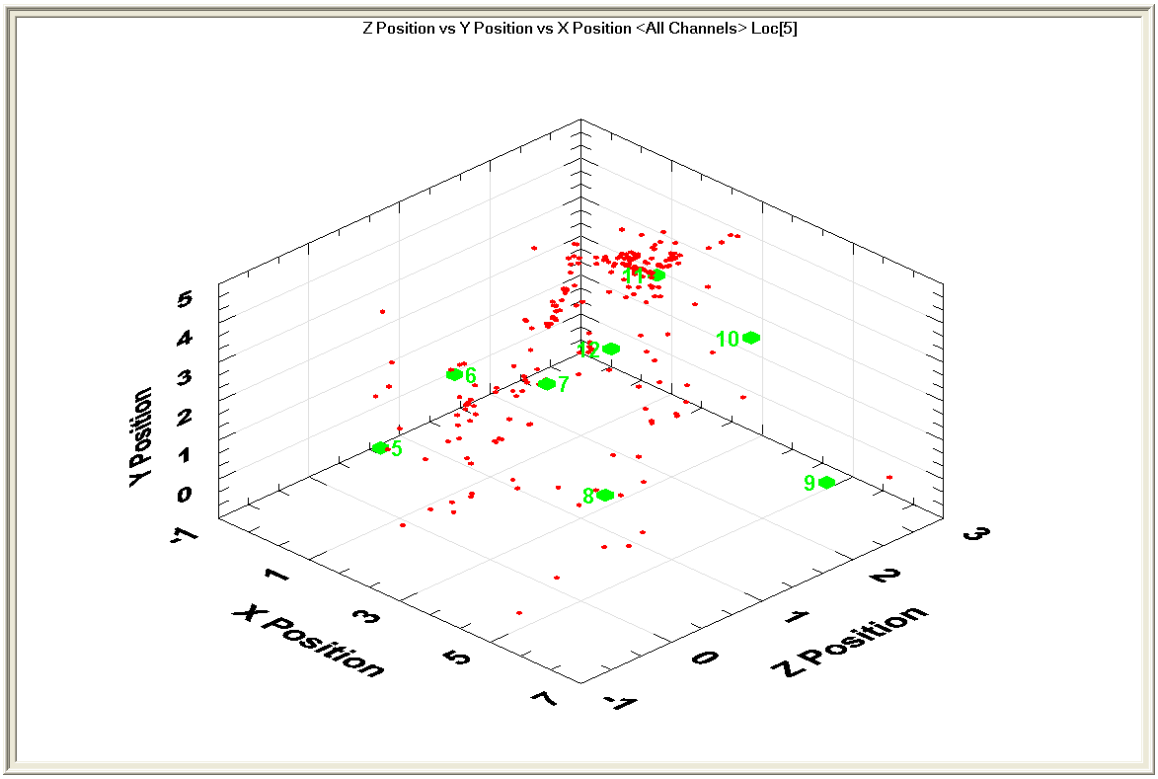

Figure 24. 3D Plot of Crack-Related AE Hits Recorded November 13-December 13, 2008, in Concrete Structure Under Cable Saddle. The coordinates (X,Y,Z) are defined in Figure 22.

Both plots establish the existence of a heavy concentration of AE activity in the region between Sensor 6 on the west face and Sensor 11 on the east face. These plots also establish the existence of crack-related AE activity in the larger area of the saddle structure, a fact that could not be established by 2D analysis. The analysis of AE signal amplitudes and sensor coordinates bore out the fact that of 743 hits near Sensor 11, only 147 were above the minimum energy of cracking (75 energy counts) and of 147 significant hits, only 3 were related with cracking; the rest were related with rubbing (friction). Accordingly, ~98% of the AE activity was related with crack friction and ~2% with cracking through microbursts. Further, the crack activity covered both the width and the depth of the saddle, being larger near the surface in comparison to that in the bulk. The new cracks seemed to initiate on the surface and grow in length, width, and depth with time, resulting in the increase of crack growth toward the bulk.

Field Inspection of Pylon Saddle Area

Based on the results of AE events and their analysis, on-site inspections of the saddle area were conducted for physical verification. Physical verification confirmed the growth of the pre-existing cracks and initiation of new cracks in the concrete structure of the saddle walls. A schematic of the areas of the locations of cracks is shown in Figure 25. Physical verification revealed pre-existing (shown as marked on Figure 25) and new cracks on the saddle walls. The crack sizes in different locations were measured, as shown on Figures 26 and 27 and summarized in Tables 9 and 10. Figure 28 shows photographs of some of the typical and prominent cracks in different locations of the saddle area. Based on the AE results, some of the cracks observed inside the pylon are active and have grown during the period of this study.

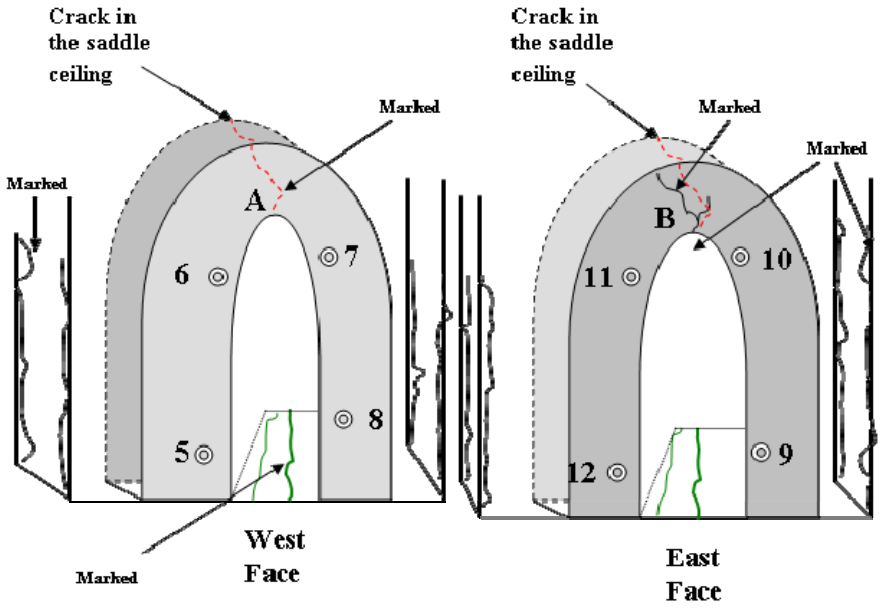

Figure 25. Cracks Detected by Sensors and Verified During Site Visit to Saddle Area. *A* and *B* are the highest points on the ceiling of the saddle. Cracks identified as "marked" were pre-existing. Unmarked cracks are new.

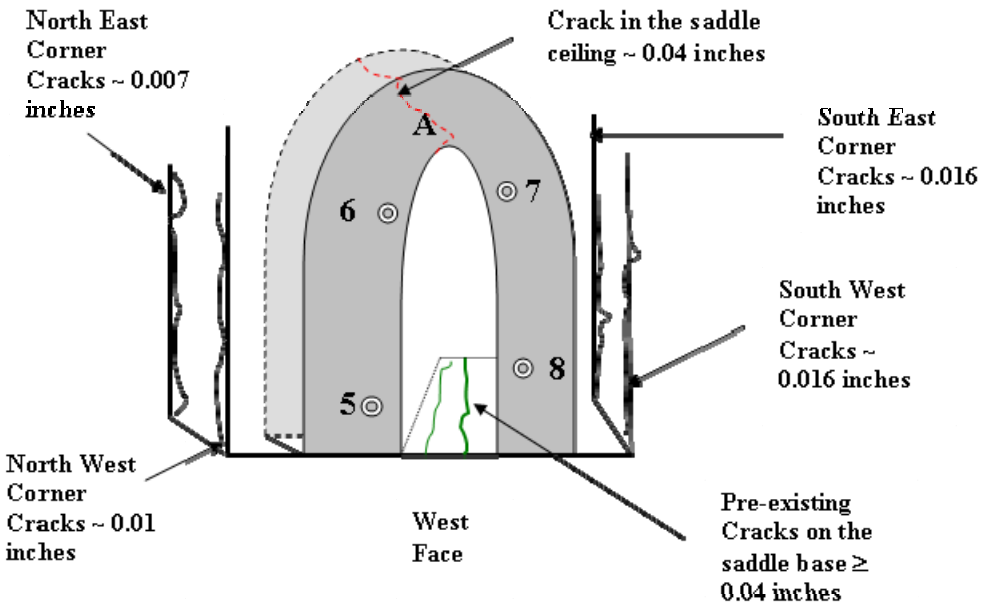

Figure 26. Cracks Detected by Sensors and Verified by Site Visit in Saddle area. *A* and *B* are the highest points on the ceiling of the saddle. Some cracks identified as "marked" were previously (before the commencement of this investigation) observed. Unmarked cracks are new. Both marked and unmarked cracks grew in size. See Table 9 for a summary of crack sizes.

Table 9. Crack Sizes (Inches) on West Side of Saddle as Shown in Figure 26

On West Face	On Ceiling of Saddle Curve	On Southeast Corner of East Face	On Southwest Corner of East Face	On Northeast Corner of East Face	On Northwest Corner of East Face
None	0.04	0.016	0.016	0.007	0.01

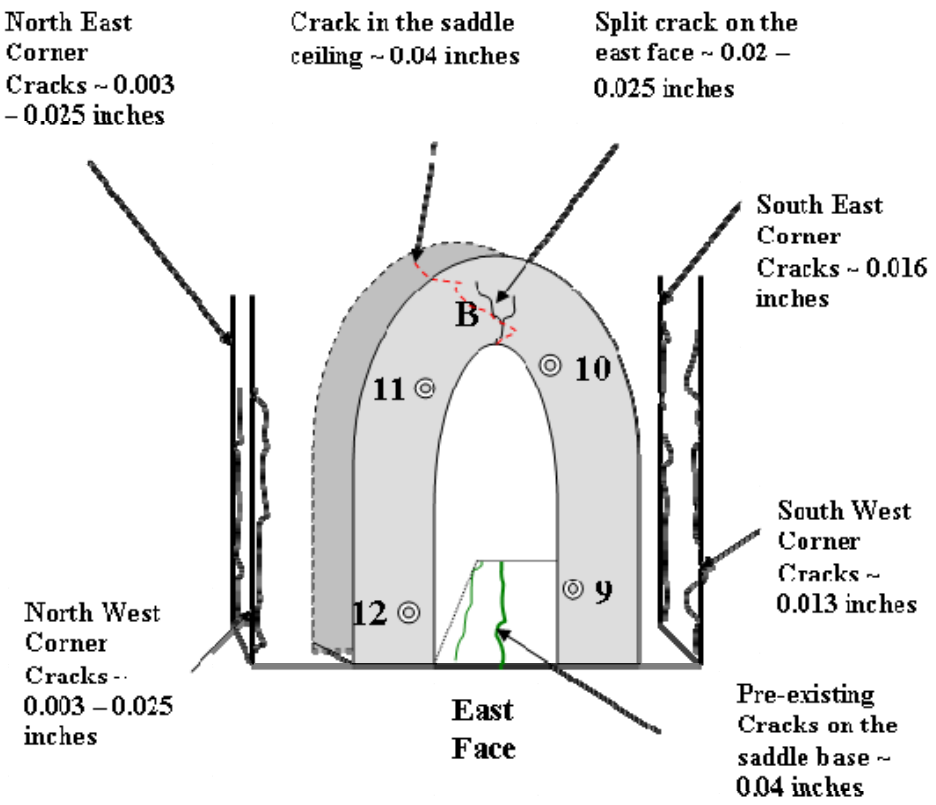

Figure 27. Cracks Detected by Sensors and Verified by Site Visit in Saddle Area. *A* and *B* are the highest points on the ceiling of the saddle. See Table 10 for a summary of crack sizes.

Table 10. Crack Sizes on East Side of Saddle As Shown in Figure 27

On East Face (Split Crack)	On Ceiling of Saddle Curve	On Southeast Corner of East Face	On Southwest Corner of East Face	On Northeast Corner of East Face	On Northeast Corner of East Face
0.02-0.025	0.04	0.016	0.013	0.003-0.025	0.003-0.025

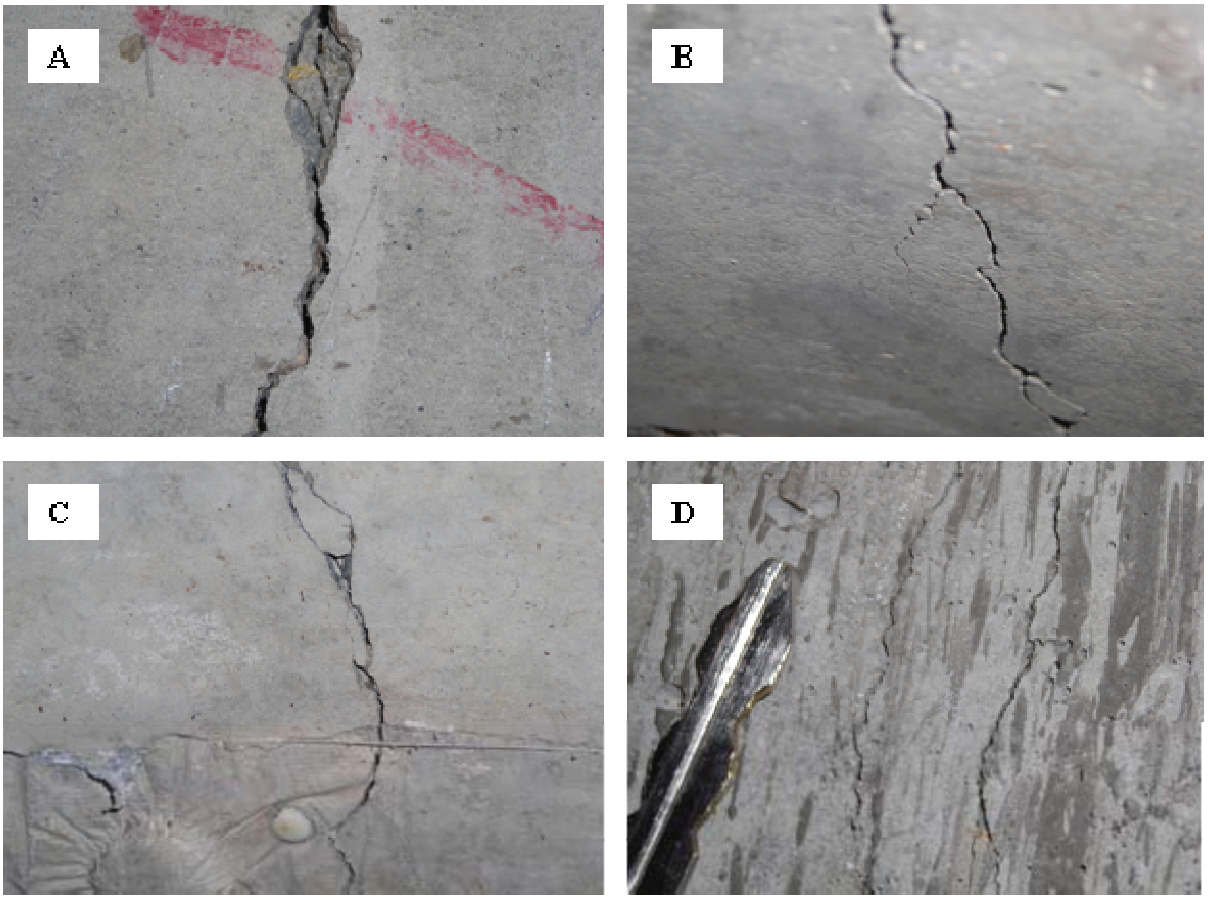

Figure 28. ***A, B, C,*** **Cracks in center of saddle ceiling;** ***D,*** **Crack on fast face of saddle.** Car key is placed for comparison of the size.

SUMMARY

- AE was successfully used on the Varina-Enon Bridge on a single stay-cable and demonstrated that AE can provide useful data as a wide area short-term (non-permanent) NDT monitoring technique.

- The study demonstrated that a 16-sensor AE DAQ (Sensor Highway II) could gather valuable information over a short period of time (2½ winter and 2½ summer months).

- AE data transmission through a broadband wireless modem installed on the DAQ system successfully provided information from the bridge to an off-site location using a Windows XP platform.

- AE data analysis software for replay of the acquired data was suitably customized for the present situation incorporating the sensor locations on the cable and in the saddle area.

- AE responses did not contain any signatures of rubbing from previously broken cable and/or breaking during the testing period. AE signals, possibly because of higher winds or blowing

debris striking the cable/anchorage region, were detected, but further investigation is required.

- Between Sensors 2 through 4 and 13 through 15, no signature sounds originating from the cable rubbing attributable to pre-existing fractures and/or cable breaks that might have occurred during the test were detected. However, the detection of feeble impacts from snowflakes and/or falling raindrops on the stay-cable surface provides strong support for the view that any active strand corrosion would have been detected and pinpointed had it existed.

- The presence of cracks at multiple locations in the saddle area, detected by the sensors, was confirmed and verified by visual observations on a site visit to the location. The cracks (both new and pre-existing) were located, and their sizes measured.

- Linear and 2D location analysis of AE data gave information on areas of active defects in concrete. A 3D analysis of the data provides more precise information on the locations and causes of the active defects. 3D analysis found that ~98% of the crack activity was due to crack rubbing (friction) and ~2% was due to crack formation (initiation). However, in view of the architectural shape of the saddle, a modification in the sensor locations will be required to meet the validity criteria for 3D analysis. A software program, such as Noesis, for pattern recognition and source classification; the filtering out of noise; and discrimination between different damage-related events, such as brittle fracture and fatigue, will have to be used. However, with the limited scope of the current study, no such pattern recognition software was used.

CONCLUSIONS

- *AE activity was occasionally detected at the sensors nearest the deck anchorage points.* This activity is unrelated to precipitation events, is inconsistent with signatures of damage, and could possibly be due to higher winds causing vibrations or blowing debris striking the cable/anchorage region. Further investigation is required, which should include redistributing some of the AE sensors to examine this region better.

- *There is AE activity in the concrete structure of the saddle area for Cable 10 on the northern pylon.*

- *AE was able to detect crack formation and growth and determine AE source locations.*

- *AE analysis identified factors related to the health of the bridge components and differentiated between those of unrelated events such as rain and snow.*

- *AE is a viable method for evaluating and/or monitoring a sizable area of the Varina-Enon Bridge and obtaining near real-time information on any activity related to its structural integrity.*

RECOMMENDATIONS

1. *VDOT's Richmond District Bridge Division should measure and map the cracks in both the northern and southern stay-cable pylons of the Varina-Enon Bridge.*

2. *VDOT's Richmond District Bridge Division should evaluate the northern pylon saddle regions using AE and determine which saddle areas show the greatest acoustical activity, with the Virginia Transportation Research Council (VTRC) providing guidance when requested.*

3. *VDOT's Richmond District Bridge Division should evaluate the stay-cable anchorage regions more closely using AE and determine the source of the AE signal detected during this study and which anchorage regions show the greatest acoustical activity.* VTRC should provide guidance for this recommendation when requested.

4. *VDOT's Richmond District Bridge Division should consider using AE periodically to evaluate the health of this structure and determine which regions are exhibiting the greatest AE activity.* Regions with elevated AE activity should take precedence over non-active regions during inspection. VTRC should provide guidance for this recommendation when requested.

BENEFITS AND IMPLEMENTATION PROSPECTS

In July 1990, when construction was completed, the reported cost of construction of the Varina-Enon Bridge was $34.4 million.[4] VDOT has earned seven design awards for this bridge.[4] Therefore, the bridge has both a monetary and an aesthetic value. With this in mind, it is imperative that VDOT have the tools it needs to maintain such a costly signature structure.

Unfortunately, inspection of important regions of this structure can be difficult at best. This is because the technique for protecting the steel is to embed it in concrete, encase it in plastic, or both. Therefore, as shown in Figure 29, to inspect a wire strand usually involves the removal of these protective layers, with the location for inspections often based on an assumption of where a problem might exist. This method creates the potential for missing unexpected damage, since it is based on historical data, experience, and probability rather than technology that characterizes the condition of the part or assembly of interest. Moreover, the removal of the protective materials can be destructive, so the area inspected must be repaired.

It is also important to mention that other nondestructive techniques have been or are being developed with the purpose of assessing the condition of important structural components. For example, one approach generates condition data using magnetic fields and looks promising for evaluating stay-cables or exposed tendons; however, employment of the results of this technique to evaluate deviator blocks and anchorage regions is still not field ready. This is where techniques such as AE are comparatively advantageous because AE can evaluate all of these areas mentioned and is field ready. AE complements several other nondestructive techniques, which, when used in conjunction, would most likely provide the best diagnostic option.

Figure 29. ***Top Left,*** **Stay-cable prior to inspection;** ***Top Right,*** **Rubber boot removed and inspection location determined;** ***Middle Left, Middle Right, and Bottom Left,*** **Plastic removed to create portal for viewing;** ***Bottom Right,*** **Viewing portal opened and wires revealed for inspection.**

This study demonstrated that in bridge elements that would otherwise be difficult if not impossible to evaluate nondestructively, AE provides a useful means for determining areas of interest and insight into what is occurring. By locating the AE source and determining what is generating the source, AE can provide feedback to inspectors and engineers that surpasses traditional inspection methods. Therefore, since AE equipment is commercially available and contracts can be established to have AE services preformed, AE should be performed periodically on the Varina-Enon Bridge as indicated in the recommendations to ensure inspection provides the greatest value to VDOT.

ACKNOWLEDGMENTS

The authors appreciate the opportunity afforded by VDOT and VTRC to conduct this study. Special thanks go to Michael Sprinkel and Gary Martin for their interest, support, encouragement, and help during the entire study. The authors also thank VTRC's Cindy Perfater of the administrative staff and VTRC's Corrosion/NDE Technicians Cesar Apusen and Darren Galford for their timely help and valuable support. Thanks are also due to Terry Tamutus and Richard Gostautas of Mistra's Group for valuable and timely support in updating the instrumentation and software.

REFERENCES

1. Maddox, S.J. *Fatigue Strength of Welded Structures.* Abington Publishing, Cambridge, 1991.

2. Yuyama, S., Okamoto, T., and Nagataki, S. Acoustic Emission Evaluation of Structural Integrity in Repaired Reinforced Concrete Beams. *Materials Evaluation,* Vol. 52, No. 1, 1994, pp. 86-90.

3. Gongkang, F., ed. *Inspection and Monitoring Techniques for Bridges and Civil Structures.* CRC Press, Washington, D.C., 2005.

4. FIGG Engineering Group. http://www.figgbridge.com/varina_enon_bridge.html/. Accessed March 11, 2010.